Impact of electron–phonon coupling on the quantum yield of photovoltaic devices

Tahereh Nematiaram, Asghar Asgari, Didier Mayou

The Journal of Chemical Physics ARTICLE scitation.org/journal/jcp

Impact of electron–phonon coupling on the quantum yield of photovoltaic devices

Cite as: J. Chem. Phys. 152, 044109 (2020); doi: 10.1063/1.5140323
Submitted: 26 November 2019 • Accepted: 12 January 2020 •
Published Online: 29 January 2020

Tahereh Nematiaram,[1,2,a),b)] Asghar Asgari,[2] and Didier Mayou[1]

AFFILIATIONS

[1]Institut Néel, CNRS and Université Grenoble Alpes, Grenoble F-38042, France
[2]Research Institute for Applied Physics and Astronomy, University of Tabriz, Tabriz 51665-163, Iran

[a)]**Current address:** Department of Chemistry and Materials Innovation Factory, University of Liverpool, Liverpool L69 7ZD, U.K.
[b)]**Author to whom correspondence should be addressed:** tahereh.nematiaram@liverpool.ac.uk

ABSTRACT

In describing the charge carriers' separation mechanism in the organic solar cell, providing a method, which considers the impact of all parameters of interest on the same footing within an inexpensive numerical effort, could play an essential role. We use here a simple tight-binding model to describe the dissociation of the charge carriers and investigate their dependence on the physical parameters of the system. We demonstrate that the quantum yield of the cell is subtly controlled by the collective action of the Coulomb interaction of the electron–hole pair, electron–phonon coupling, and the geminate recombination of the charge carriers. This approach should help us understand the performance of organic solar cells and optimize their efficiency.

I. INTRODUCTION

Organic photovoltaic devices (OPVs) have triggered widespread attention in recent years due to their promising potential toward the generation of inexpensive green energy.[1–3] A significant improvement in the cell efficiency has been observed by the introduction of the bulk hetero-junction (BHJ) devices consisting of a blend film of donor (usually a polymer) and acceptor (usually fullerene derivatives) materials.[4–7] In the BHJ OPVs, an absorbed photon creates a bound electron–hole pair, the so-called exciton, which migrates to the donor–acceptor interface to be separated into free charge carriers, and is then transported toward the electrodes.[8–10] The efficiency of the device is literally controlled by the success rate of charge carriers in reaching the electrodes without recombination. The charge migration rate is determined by electron and hole mobilities, which are affected by many factors, for instance, the morphology of materials, charge carriers interactions and recombination, temperature, coupling to vibrational modes, external electrical fields, and polarization effects caused by atomic induced dipoles on adjacent molecules. Accordingly, the consideration of electron–hole interaction, geminate recombination, and electron–phonon coupling is unavoidable for a fully microscopic understanding of the charge separation mechanism in organic photovoltaic devices. To tackle this problem, various numerical methods such as exact diagonalization,[11] diagrammatic Monte Carlo,[12] time-dependent density functional theory,[13] the Dirac–Frenkel's time-dependent variational principle,[14] quantum master equation,[15] and other approaches[16–18] have been developed. However, these methods are quite demanding from a computational point of view, which makes the comprehensive treatment of the charge separation process a challenging task. In the present study, we contribute to the theory of organic photovoltaic devices, extending on various other studies addressing the problem of energy conversion in OPVs.[19–25] We develop a theoretical model that is based on the scattering theory and the Lippmann–Schwinger equation and has been employed in our recent works to assess the impact of hole propagation, off-set energies, electron–hole interaction, and non-radiative recombination on the charge separation yield.[26–29] In this work, we go a step further and study microscopically the relative role of phonons in addition to charge interaction and recombination on the quantum yield. Such modes are strongly coupled to the electronic orbitals as shown, e.g., by *ab initio* theoretical calculations[30,31] and ultrafast spectroscopic techniques,[32,33] and lead to polaron formation in the case of a sufficiently strong electron–phonon

coupling.[11,14,34] This methodology helps us understand the difference in transferring an electron to a manifold of polaronic bands rather than to a purely electronic band. It has to be noted that similar methodologies have been applied to the molecular junctions, which are comparable to the systems examined here.[35,36] In particular, the present formalism extends on previous work by Galperin and Nitzan in the context of molecular junctions[37] and by including the impact of electron–hole interaction, electron–phonon coupling and geminate recombination adds important highly non-trivial aspects to that model. Among the interesting novelties of this method compared to prior studies[11–18] is that it provides an energy domain framework which, on the one hand, enables one to have access to detailed spectral information, a suitable framework to interpret the results, and, on the other hand, provides an efficient inexpensive numerical approach to treat all parameters of interest on the same footing. The outline of this paper is as follows: In Sec. II, the theoretical model is described. Section III is divided into two parts: In Sec. III A, we investigate the cell performance in the presence of a short-range electron–hole interaction, and in Sec. III B, the impact of long-range interaction is considered. A brief summary is given in Sec. IV.

II. THEORETICAL MODEL

The following generic Hamiltonian is utilized to describe the quantum-mechanical charge transfer process of an electron at a molecular chain of length N interacting with a vibrational bath:

$$H = \varepsilon_0 c_0^+ c_0 + \sum_{l=1}^{N} \frac{V}{l} c_l^+ c_l + C\left(c_0^+ c_1 + c_1^+ c_0\right) + J\sum_{l=1}^{N}\left(c_l^+ c_{l+1} + c_{l+1}^+ c_l\right) + \hbar\omega_0 \sum_{l=1}^{N} a_l^+ a_l + g\sum_{l=1}^{N} c_l^+ c_l\left(a_l^+ + a_l\right), \quad (1)$$

where $a_l^+(a_l)$ and $c_l^+(c_l)$ are the phonon and electron creation (annihilation) operators on site l, respectively, $\hbar\omega_0$ represents the energy of the relevant molecular vibration, g is the local electron–phonon coupling constant, C is the tunneling amplitude between the donor (site $l = 0$) and the first site of the tight-binding chain describing the acceptor (site $l = 1$), ε_0 is the energy of the incoming electron, V sets the typical Coulomb potential binding the electron–hole pair, and J is the transfer integral between adjacent molecules within the acceptor chain (sites $l = 1{:}N$). In the following, to outline the strength of the local electron–phonon coupling, we use the dimensionless Huang–Rhys parameter $\alpha^2 = (g/\hbar\omega_0)^2$, which is a ratio between the molecular reorganization energy and the phonon energy.[38]

Our main assumptions in this study are as follows: (i) we assume that the hole is fixed in the interface (at site $l = 0$); however, the effects of hole diffusion can be described by a reduction in the effective Coulomb binding and can be easily taken into account by extending the Hamiltonian in Eq. (1).[29] (ii) A single intramolecular mode of vibration is considered. The multiple phonon modes provide additional transfer channels and treating them properly requires a detailed knowledge of all the modes which is not the focus of present study. (iii) A Coulomb potential for the electron–hole is considered, although other types of interaction should not cause drastic changes in the results.[39,40] (iv) We study the model at the zero temperature. This assumption is justified as the electronic and vibrational energies are much larger than k_BT. (v) For simplicity, we consider only the momentum average treatment of the model as such the phonon modes are excited only on the site where the electron arrives and all the other modes are empty. Although the momentum average approximation neglects the inelastic processes, it provides a suitable framework to describe the polaronic bands.

Starting from the quantum scattering theory and Lipmann–Schwinger equation,[28] we introduce the local polaronic Green's function at site $l = 0$ (see the supplementary material for further details) or the so-called resolvent,

$$G_0(z) = \left(z - \varepsilon_0 + i\frac{\Gamma_R}{2} - C^2\tilde{G}_1(z)\right)^{-1}, \quad (2)$$

with z and Γ_R being a complex energy with an infinitesimal positive imaginary part and the geminate recombination parameter, respectively. $\tilde{G}_n(z)$ denotes the Green's function on site n when all sites between n and 0 are neglected and obey a recurrence relation as follows:

$$\tilde{G}_n(z) = \left(z - \frac{V}{n} - \Sigma_p(z) - J^2\tilde{G}_{n+1}(z)\right)^{-1}, \quad (3)$$

where $\Sigma_p(z)$ is the so-called phonon self-energy, which can be computed according to the phonon chain Green's function as explained in detail in the supplementary material. The so-called polaronic Green's function $G_0(z)$ in the absence of coupling to the phonon modes is the retarded Green's function for a single electron. As shown in Ref. 28, having defined the $G_0(z)$ enables one to investigate the quantum yield Y, which is a manifestation of competition between electronic motion and loss processes (e.g., charge carriers recombination),

$$Y = \int \frac{-C^2\,\mathrm{Im}\,\tilde{G}_1(z)}{\left(\frac{\Gamma_R}{2} - C^2\,\mathrm{Im}\,\tilde{G}_1(z)\right)} \times n_0(z)dz, \quad (4)$$

where $n_0(z) = -(1/\pi)\,\mathrm{Im}\,G_0(z)$ is the density of states (DOS) on site $l = 0$. It has to be noted that when the recombination parameter Γ_R tends to zero, only the energies leading to nonzero $\mathrm{Im}\,\tilde{G}_1(z)$, i.e., the energies in the continuum contribute to the yield. In that case, one obtains $Y = 1 - P$ where $P = 1 - \int n_0(z)dz$ denotes the weight of localized states on the initial state $l = 0$. Indeed, the part of the initial wave-function that decomposes on localized states stays close to the interface until it undergoes recombination even in the case of the insignificant recombination parameter. On the contrary, the part which decomposes on eigen-states of the continuum gets the opportunity of injection to the electrodes if Γ_R tends to zero. Let us emphasize that in a solar cell, there is also the question of how the electron goes to the electrode which requires an electric field that can be self-consistent with the flow of charge and may modify the local Hamiltonian. The results presented here do not treat the effect of an external varying voltage. In that sense, we are not presenting a full theory of organic solar cells. Yet the present work sheds light on basic quantum phenomena that occur in this type of cell.

III. RESULTS AND DISCUSSIONS

In the following, we examine the density of states and the charge separation yield. The initial state in the model consists of an electron injected on the donor site $l = 0$ with excess energy ε_0, without any coupling to the phonon modes. All the vibration modes on the acceptor chain are empty. We set the basic energy unit to be the hopping parameter on the sites of acceptor material $J = 1$. The donor to acceptor tunneling rate is set to $C = 0.5$. The values of J and C are chosen to be different as the former stands for the coupling between the molecules of the same material (acceptor) while the latter denotes the coupling between the molecules of different materials (donor and acceptor). The vibration frequency is also set to $\hbar\omega_0 = 1$. All the parameters are expressed as a factor of J; however, as long as the calculation is done in the non-adiabatic regime (i.e., $\hbar\omega_0 \geq J$),[41] the precise values are not so important. The other three parameters, i.e., the injection energy ε_0, the local electron–phonon coupling α^2, and the strength of the Coulomb potential V are kept free. In the following, considering the local electron–phonon coupling, we assess the density of states and the quantum yield in the presence of (Sec. III A) a short-range electron–hole interaction and (Sec. III B) a long-range electron–hole interaction.

A. Short-range electron-hole interaction

The short-range interaction term indicates that the electron–hole interaction occurs only on the site $l = 0$ whose effect is no more than a change in the onsite energy of this site (ε_0). The local density of states (DOS) far from the interface (the so-called bulk part) is an essential parameter, which reveals the influence of intramolecular vibrations on the electronic structure. We compute the local DOS for different strengths of electron–phonon coupling. As shown in Fig. 1, a series of bands appears at the edges, which are the so-called polaronic bands. In the limit studied here, there is essentially no scattering effect by the phonons, and therefore, the coupling to the phonon modes mainly causes the band renormalization. The gaps between the different bands of the local DOS spectrum appear as a result of resonance energies caused by the coupling to the phonon modes. Mathematically, these gaps appear when the phonon self-energy $\Sigma_p(z)$ diverges or equivalently when the polaron Green's function $G_0(z)$ becomes zero. It has to be noted that there is an infinite number of polaronic bands which are centered around energies given by $\hbar\omega_0(m - \alpha^2)$. However, the amplitude of the polaronic peaks decrease with $1/m!$ (m is the number of polaronic peaks), and therefore, all the peaks cannot be observed in Fig. 1. The spectrum of the polaronic bands can be obtained straightforwardly from $\tilde{G}_n(z)$ at a large n. Indeed, the spectrum corresponds to energies for which $\tilde{G}_n(z)$ have a non-zero imaginary part implying that the effective energy $z - \Sigma_p(z)$ belongs to the spectrum of the bare electron chain (i.e., no coupling to phonon modes), which is extended in the energy interval of $[-2J, 2J]$.

To evaluate the charge separation yield in the presence of electron–phonon coupling and local Coulomb interaction (second row in Fig. 1), we begin by considering the case without charge carrier recombination ($\Gamma_R = 0$), scanning for all possible values of the injection energy ε_0 and varying the strength of the electron–phonon coupling α. We find that in the non-interacting and non-recombining electron–hole conditions, the yield within the acceptor bandwidth, i.e., $-2J \leq \varepsilon_0 \leq 2J$, is one as long as $\alpha = 0$. Upon

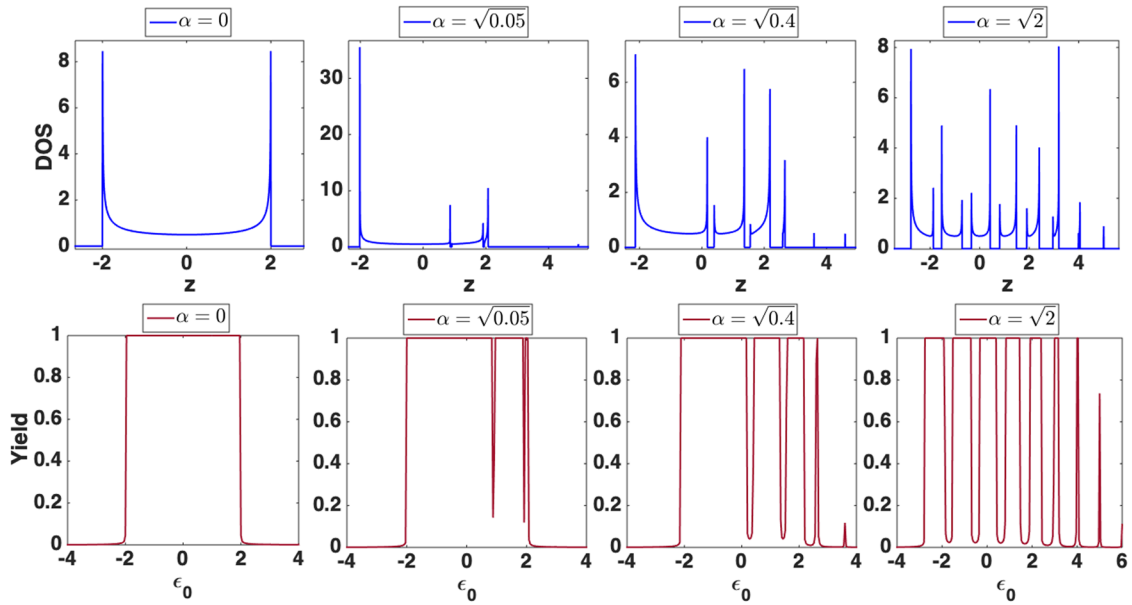

FIG. 1. Top panels: the local density of states in the bulk part for different strengths of electron–phonon coupling α showing the polaronic bands. Bottom panels: the charge separation yield as a function of injection energy ε_0 in the presence of local electron–hole Coulomb interaction and for various values of α. The figures are obtained for $\hbar\omega_0 = J = 1$.

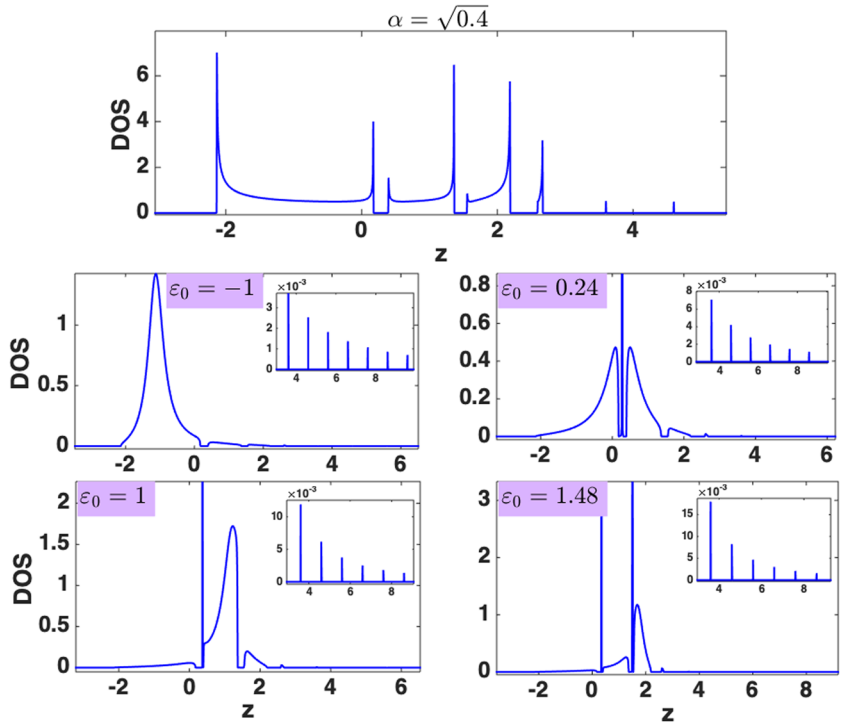

FIG. 2. From top to the bottom: local density of states in the bulk part and close to the interface for different injection energies. The electron–phonon coupling constant is set to $\alpha = \sqrt{0.4}$. All the energies are expressed in terms of J as the basic energy unit.

increasing α, several sub-bands appear, which are in conformity with the polaronic band structure of the acceptor side[42] shown in the top panels of the same figure. As can be seen for any value of α, one can find energy bands where the yield is almost one, indicating that polarons behave like "good" charge carriers. An in depth analysis of the spectral information enables one to understand the required conditions for the efficient charge extraction and consequently the higher yield. Therefore, in Fig. 2, for an arbitrary α, we examine the

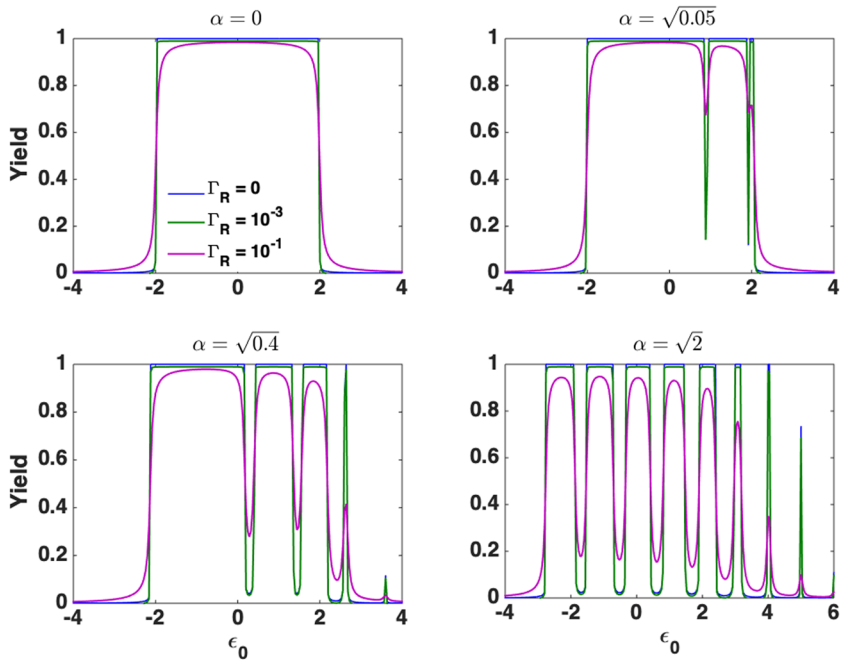

FIG. 3. Yield as a function of injection energy ε_0 for various values of the electron–phonon coupling constant α and electron–hole recombination parameter Γ_R. The legend presented in the first panel is valid for all the other panels. All the energies are expressed in terms of J as the basic energy unit.

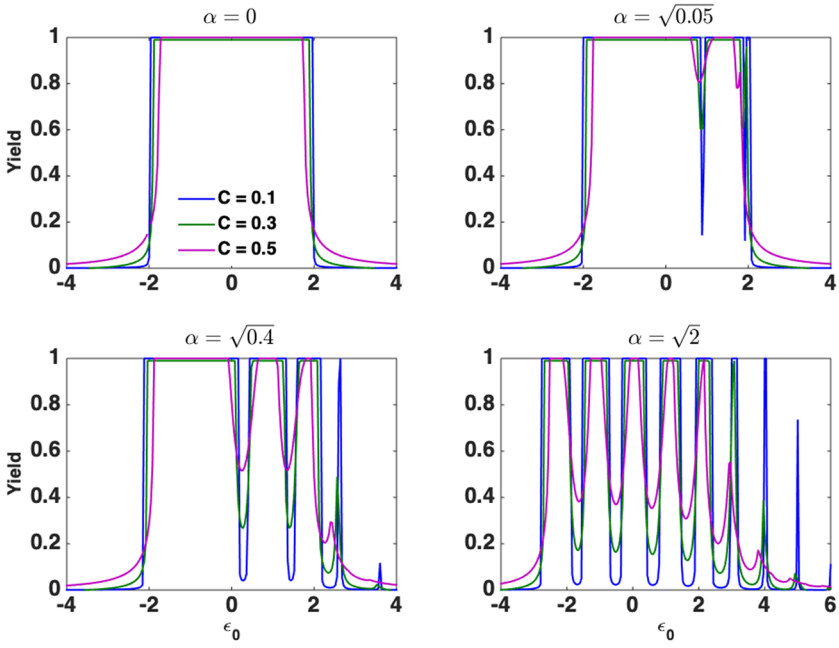

FIG. 4. Yield as a function of injection energy ε_0 for various values of the electron–phonon coupling parameter α and electronic coupling C. The legend presented in the first panel is valid for all the other panels.

density of states in the bulk (far from the interface) and also close to the interface for different injection energies ε_0. The electronic structure in the bulk part represents an aggregate picture of all possible polaronic bands and the energy gap regimes. As depicted in the four bottom panels, for a given injection energy ε_0, the electronic structure may contain the energy states on the "allowed" polaronic bands or contrarily on the localized states in the energy gap (defined on the basis of bulk DOS). The charge carriers lying in a polaronic band can evacuate and reach the electrodes, and conversely, the ones localized in the bound state in the gap regimes recombine quickly, leading to a reduction in the yield. Here, we draw the reader's attention to a delicate point: as can be seen, for injection energies well above the band of the bare electron chain ($+2J$), the yield never reaches one. At a large band index m, i.e., in the regime of high orbital energy, the width of the polaronic band is so narrow such that the coupling of the interface LUMO to this band is stronger than the width of

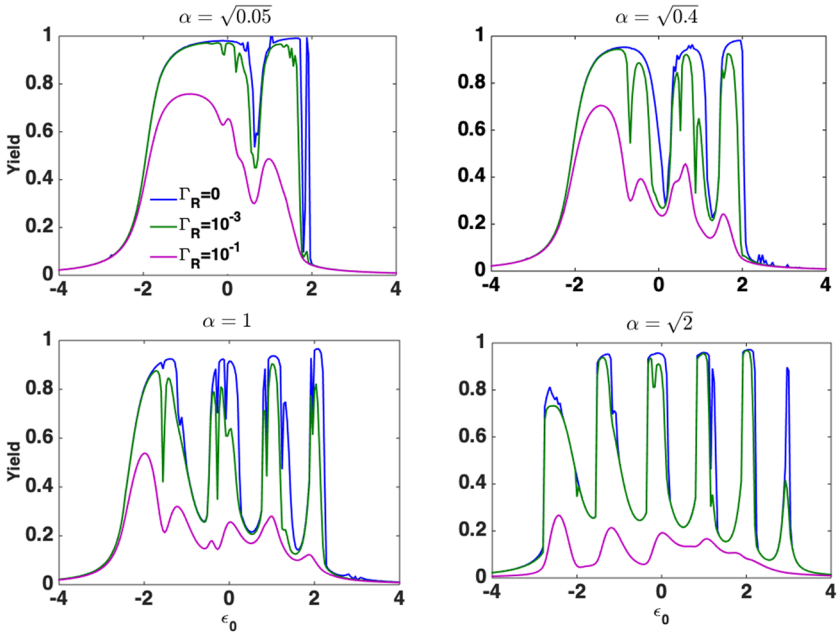

FIG. 5. Yield as a function of injection energy ε_0 for various values of the electron–phonon coupling α in the presence of long-range electron–hole binding $V = -1$ and different electron–hole recombination parameters Γ_R. The legend presented in the first panel is valid for all the other panels.

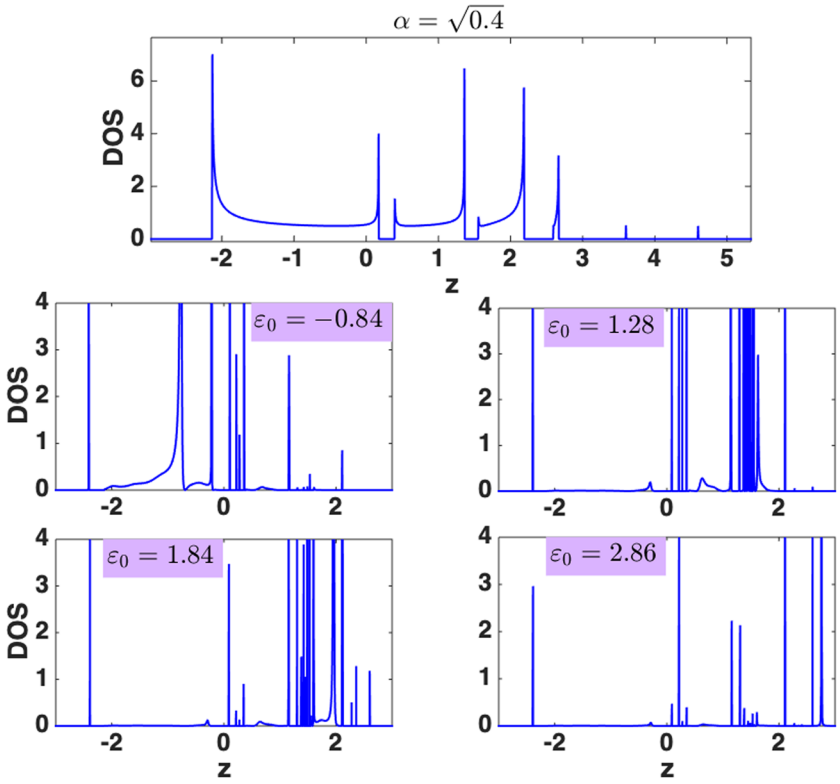

FIG. 6. Local density of states in the bulk part and close to the interface for different injection energies. The electron–phonon coupling constant is set to $\alpha = \sqrt{0.4}$, and Coulomb interaction energy is $V = -1$.

the band. Therefore, a localized state exists regardless of the initial orbital energy. Since there is always a localized polaronic state, the bound electron–hole pair ultimately recombines and the yield never reaches one in this regime.

For further investigation, in Figs. 3 and 4, we investigate the effects of the recombination parameter Γ_R and tunneling amplitude C on the charge separation yield. The charge carrier recombination reduces the probability of charge separation and, as can be seen, it leads to a reduction in the yield, which gets more significant in the presence of stronger electron–phonon coupling. On the other hand, a stronger tunneling parameter C facilitates the electron injection to the acceptor band, and as can be seen from Fig. 4, the yield grows with increasing values of C as long as the injection energy does not fall within the strong coupling limit where bound states appear leading to charge carriers recombination and yield reduction.

B. Long-range electron–hole interaction

In this stage, the former evaluations are repeated for the case of long-range Coulomb interaction. The strength of Coulomb interaction is assumed to be $V = -1$ and its impact in the presence of recombination and local electron–phonon coupling is depicted in Fig. 5. The following points are remarkable: First, the yield keeps the periodic resonance structure as a consequence of polaronic band formation. Second, for all values of α, the combined effect of Coulomb interaction and polaronic dressing of the carriers leads to a strong overall suppression of the yield such that it never reaches one. Third, with increasing α, the yield drops down even in the regime of bare electron spectrum (i.e., the energy interval $[-2J, 2J]$), which is not observed in the absence of long-range Coulomb interaction. Fourth, as before, the effects of recombination Γ_R can be detected through a global reduction of the yield, although its impact is more significant in the presence of long-range Coulomb interaction.

The spectral information represented in Fig. 6, which is obtained for an electron–phonon coupling strength $\alpha = \sqrt{0.4}$, facilitates the rationalization of the yield behavior. We find that the long-range Coulomb interaction leads to a more intricate spectrum with many localized and nearly localized states, which further reduce the charge separation yield.

IV. CONCLUSIONS

We present that the charge separation yield in OPVs is subtly controlled by the interplay of Coulombic confinement and coherent electron–phonon coupling, which develops a methodology that is able to rationalize the difference in transferring an electron to a manifold of polaronic bands rather than to a purely electronic band. The method is developed in the energy domain and, therefore, provides spectral information to interpret the results and rationalize the oscillatory behavior of the charge separation yield. This methodology can also be applied to other light harvesting systems where there is coupling to high-frequency vibrational modes.

SUPPLEMENTARY MATERIAL

See the supplementary material for further details on derivation of the polaronic Green's function and spectrum of polaronic bands.

ACKNOWLEDGMENTS

The authors would like to thank Professor Alessandro Troisi and Dr. Simone Fratini for the useful discussions.

REFERENCES

[1] D. Baran, R. S. Ashraf, D. A. Hanifi, M. Abdelsamie, N. Gasparini, J. A. Röhr, S. Holliday, A. Wadsworth, S. Lockett, M. Neophytou, C. J. M. Emmott, J. Nelson, C. J. Brabec, A. Amassian, A. Salleo, T. Kirchartz, J. R. Durrant, and I. McCulloch, Nat. Mater. **16**, 363 (2017).
[2] P. Cheng, G. Li, X. Zhan, and Y. Yang, Nat. Photonics **12**, 131 (2018).
[3] M. Grätzel, J. Photochem. Photobiol. C Photochem. Rev. **4**, 145 (2003).
[4] G. Zhang, J. Zhao, P. C. Y. Chow, K. Jiang, J. Zhang, Z. Zhu, J. Zhang, F. Huang, and H. Yan, Chem. Rev. **118**, 3447 (2018).
[5] W. Yang, Z. Ye, T. Liang, J. Ye, and H. Chen, Sol. Energy Mater. Sol. Cells **190**, 75 (2019).
[6] J. K. Lee, W. L. Ma, C. J. Brabec, J. Yuen, J. S. Moon, J. Y. Kim, K. Lee, G. C. Bazan, and A. J. Heeger, J. Am. Chem. Soc. **130**, 3619 (2008).
[7] N. Sergeeva, S. Ullbrich, A. Hofacker, C. Koerner, and K. Leo, Phys. Rev. Appl. **9**, 024039 (2018).
[8] M. Einax and A. Nitzan, J. Phys. Chem. C **118**, 27226 (2014).
[9] M. Einax, M. Dierl, and A. Nitzan, J. Phys. Chem. C **115**, 21396 (2011).
[10] K. Beltako, F. Michelini, N. Cavassilas, and L. Raymond, J. Chem. Phys. **148**, 104301 (2018).
[11] G. Wellein and H. Fehske, Phys. Rev. B **56**, 4513 (1997).
[12] P. E. Kornilovitch, Phys. Rev. Lett. **81**, 5382 (1998).
[13] C. Andrea Rozzi, S. Maria Falke, N. Spallanzani, A. Rubio, E. Molinari, D. Brida, M. Maiuri, G. Cerullo, H. Schramm, J. Christoffers, and C. Lienau, Nat. Commun. **4**, 1602 (2013).
[14] S. Bera, N. Gheeraert, S. Fratini, S. Ciuchi, and S. Florens, Phys. Rev. B **91**, 041107 (2015).
[15] G. Li, Phys. Chem. Chem. Phys. **17**, 11553 (2015).
[16] S. L. Smith and A. W. Chin, Phys. Rev. B **91**, 201302 (2015).
[17] Y. Yao, New J. Phys. **19**, 043015 (2017).
[18] H.-G. Duan, A. Jha, V. Tiwari, R. J. D. Miller, and M. Thorwart, Chem. Phys. **528**, 110525 (2020).
[19] M. Ernzerhof, M.-A. Bélanger, D. Mayou, and T. Nemati Aram, J. Chem. Phys. **144**, 134102 (2016).
[20] R. A. J. Janssen and J. Nelson, Adv. Mater. **25**, 1847 (2013).
[21] G. Li, A. Nitzan, and M. A. Ratner, Phys. Chem. Chem. Phys. **14**, 14270 (2012).
[22] D. Padula, Ö. H. Omar, T. Nematiaram, and A. Troisi, Energy Environ. Sci. **12**, 2412 (2019).
[23] V. Lemaur, M. Steel, D. Beljonne, J.-L. Brédas, and J. Cornil, J. Am. Chem. Soc. **127**, 6077 (2005).
[24] A. J. White, U. Peskin, and M. Galperin, Phys. Rev. B **88**, 205424 (2013).
[25] M. Einax, M. Dierl, P. R. Schiff, and A. Nitzan, Europhys. Lett. **104**, 40002 (2013).
[26] T. N. Aram, M. Ernzerhof, A. Asgari, and D. Mayou, J. Chem. Phys. **149**, 064102 (2018).
[27] T. Nemati Aram, M. Ernzerhof, A. Asgari, and D. Mayou, J. Chem. Phys. **146**, 034103 (2017).
[28] T. Nemati Aram, P. Anghel-Vasilescu, A. Asgari, M. Ernzerhof, and D. Mayou, J. Chem. Phys. **145**, 124116 (2016).
[29] T. N. Aram, A. Asgari, and D. Mayou, Europhys. Lett. **115**, 18003 (2016).
[30] A. Troisi and G. Orlandi, J. Phys. Chem. B **109**, 1849 (2005).
[31] R. Sikora, J. Phys. Chem. Solids **66**, 1069 (2005).
[32] Y. Song, S. N. Clafton, R. D. Pensack, T. W. Kee, and G. D. Scholes, Nat. Commun. **5**, 4933 (2014).
[33] C. Yan, S. Barlow, Z. Wang, H. Yan, A. K.-Y. Jen, S. R. Marder, and X. Zhan, Nat. Rev. Mater. **3**, 18003 (2018).
[34] A. Troisi, Chem. Soc. Rev. **40**, 2347 (2011).
[35] S. N. Yaliraki, A. E. Roitberg, C. Gonzalez, V. Mujica, and M. A. Ratner, J. Chem. Phys. **111**, 6997 (1999).
[36] T. Markussen, R. Stadler, and K. S. Thygesen, Nano Lett. **10**, 4260 (2010).
[37] M. Galperin and A. Nitzan, Phys. Rev. Lett. **95**, 206802 (2005).
[38] M. Malagoli, V. Coropceanu, D. A. da Silva Filho, and J. L. Brédas, J. Chem. Phys. **120**, 7490 (2004).
[39] I. Duchemin and X. Blase, Phys. Rev. B **87**, 245412 (2013).
[40] H. Tamura and I. Burghardt, J. Phys. Chem. C **117**, 15020 (2013).
[41] M. Capone, S. Ciuchi, and C. Grimaldi, Europhys. Lett. **42**, 523 (1998).
[42] S. Ciuchi, F. de Pasquale, S. Fratini, and D. Feinberg, Phys. Rev. B **56**, 4494 (1997).